ACS OMEGA

Article

Cite This: ACS Omega 2018, 3, 5111−5115

Chromium(II) Hexacyanoferrate-Based Thin Films as a Material for Aqueous Alkali Metal Cation Batteries

Radu Bors,[†] Jeongsik Yun,[†,‡] Philipp Marzak,[†,‡] Johannes Fichtner,[†] Daniel Scieszka,[†,‡] and Aliaksandr S. Bandarenka*[,†,‡]

[†]Department of Physics, ECS, Technical University of Munich, James-Franck-Straße 1, 85748 Garching, Germany
[‡]Nanosystems Initiative Munich (NIM), Schellingstraße 4, 80799 Munich, Germany

ABSTRACT: Identification and characterization of novel battery electrode materials are key factors in transitioning the grids to renewable energy provision. Given the scale of the challenge, special attention should be paid to safety and availability of resources. This paper presents a new electrode material for aqueous batteries and supercapacitors based on highly available resources: chromium(II) hexacyanoferrate (CrHCF) thin films. Electrodeposited CrHCF exhibited "half-charge" potentials ($E_{1/2}$) of ∼0.69 and ∼0.72 V versus silver/silver chloride (reference electrode) for Na and K intercalation, respectively, a high specific capacity of ∼88 mA h/g (10 C), and a good rate performance at fast C-rate (360 C). The electrolyte composition significantly influences the long-term cycling stability of the CrHCF electrodes and the choice of the intercalating alkali metal cations significantly impacts the $E_{1/2}$ potentials. Finally, a CrHCF-based symmetric cell (quasi-supercapacitor) was constructed and showed high specific energy of ∼4.6 W h/kg at 100 C.

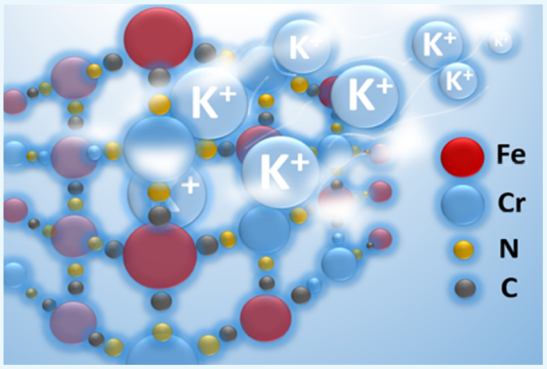

INTRODUCTION

The changes in society's perspective on climate change and sustainability have led to global compromises to reduce carbon-based emissions, such as the Paris climate change agreement. In a bid to cut carbon emission, various technologies have been developed for electricity provision from renewable energy sources, as well as for energy consumption, such as fuel cell cars and battery electric vehicles. In research and development of energy technologies, batteries (often combined with supercapacitors) are placed as the key candidates for electricity storage to transfer energy from production to consumption.[1,2] The expectation for the huge growth in the electric vehicle market has opened explosive increase of investments on battery development from both public and private institutions, leading to already successful commercialization.[3]

However, the development of appropriate electrochemical energy storage systems (ESSs) for grid ESSs is still at an early stage because of different requirements from mobile applications.[4] For large-scale applications, safety and costs should be considered to be equal to or even more important than energy density. The global energy demand is predicted to increase to ca. 30 TW_{avg} by 2050.[5] To achieve sustainable energy provision using new schemes, the availability and the abundance of materials should be taken into consideration as one of the main factors for upscaling. Figure 1 provides a visual comparison of the annual global production of common elements for battery materials. It suggests that the direct application of current Li-ion batteries onto grid-scale storage systems might not be achievable within a reasonable time scale,[5] despite their high energy density and well-developed technology. The limited availability and increasing demand of Li will further increase the price, which makes it more difficult to address the "Terawatt Challenge" in time.[6,7] Furthermore, flammable organic electrolytes of Li-ion batteries largely increase safety risks in large-scale applications.

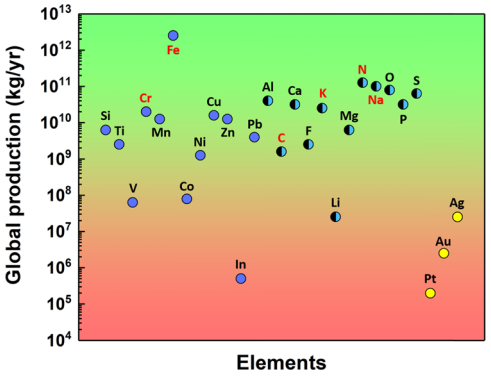

Figure 1. Annual global production of common elements for battery applications. The full circles represent the elements mainly used for electrode materials and the half-black circles represent those for either electrodes or electrolytes, partly adapted from ref 5.

Received: February 14, 2018
Accepted: April 5, 2018
Published: May 10, 2018

DOI: 10.1021/acsomega.8b00273
ACS Omega 2018, 3, 5111−5115

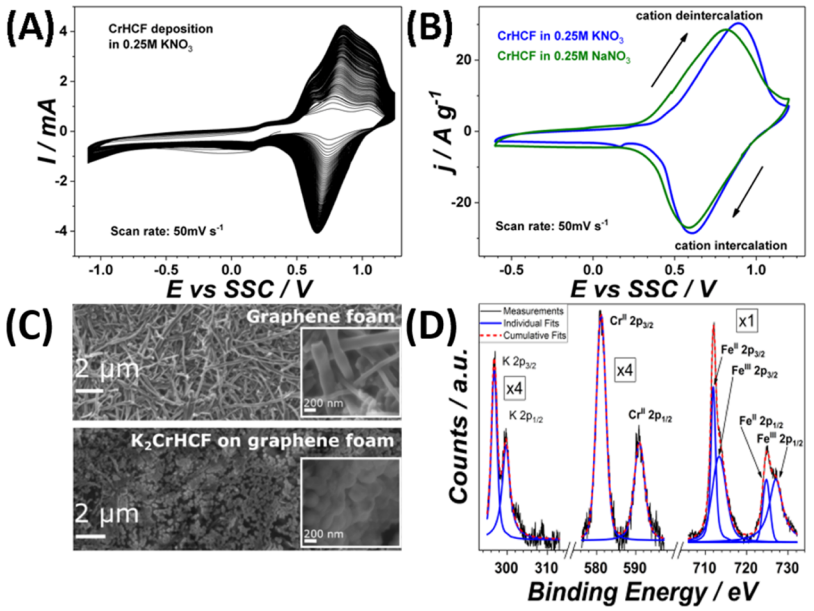

Figure 2. (A) Typical CVs characterizing the electrodeposition of CrHCF thin films. (B) Typical CVs of CrHCF thin film in aqueous 0.25 M KNO_3 (blue curve) and 0.25 M $NaNO_3$ (green curve) electrolytes. (C) SEM images of graphene foam before CrHCF deposition (top) and electrodeposited CrHCF thin films on graphene foam, showing the film morphology (bottom). (D) Typical XPS spectrum of electrodeposited CrHCF thin films. To improve the signal intensity, the CrHCF thin film was electrodeposited onto a Pt/Ti quartz crystal substrate.

Aqueous batteries using different alkali metal cations for grid-scale energy storage have drawn a considerable attention, thanks to safety and the high rate capability of aqueous electrolytes compared to organic electrolytes.[8] Among various classes of electrode materials for aqueous batteries, Prussian blue analogues (PBAs) are particularly interesting owing to their superior cycle life, low price, and abundant raw materials for building electrodes.[9−11] PBAs have fcc structure based on the two transition metals that are coordinated with sixfold carbon or nitrogen. The representative chemical formula of PBAs can be written as $X_yTM^1[TM^2(CN)_6]$ (where X represents the intercalating cations, TM^1 and TM^2 are the transition metals, and y is frequently 1 or 2). Many different PBAs have been studied for aqueous and nonaqueous batteries such as $Na_2Ni[Fe(CN)_6]$ (NiHCF),[12−14] $Na_{1.54}Co[Fe(CN)_6]_{0.86}\cdot\gamma_{0.14}\cdot 2.16H_2O$ (CoHCF),[15] $K_{0.71}Cu\ [Fe(CN)_6]_{0.72}\cdot 3.7H_2O$ (CuHCF),[16] $Na_2VO_x[Fe(CN)_6]$ (VHCF),[17] and $Na_xMn[Mn(CN)_6]$ (MnHCM).[18,19] However, considering utilization for large-scale applications and the availability of raw materials, it would be ideal to use the most abundant and light TM^1 and TM^2, namely, Cr and Fe (see Figure 1).

RESULTS AND DISCUSSION

Figure 2A shows a typical cyclic voltammogram (CV) characterizing the electrochemical deposition of chromium(II) hexacyanoferrate (CrHCF) thin films: the increase in cathodic and anodic current peaks reveals the growth of the film. Electrodeposition on graphene foam using a smaller potential range, for example, from −0.7 to 1.1 V versus silver/silver chloride (SSC), could not be achieved. Only when the lower potential was extended to −1.1 V versus SSC, CrHCF electrodeposition occurred. This is in good accordance with the claims of Gao and Jiang et al.[20,21] that reduction of Cr^{3+} (−0.95 V vs SSC)[22] is a mandatory condition for electrodeposition. Further insight into the CrHCF electrodeposition mechanism is beyond the scope of this manuscript.

Representative CVs of CrHCF thin films in aqueous 0.25 M $NaNO_3$ (green curves) and 0.25 M KNO_3 (blue curves) electrolytes characterizing intercalation and deintercalation of K^+ are depicted in Figure 2B. The cathodic and anodic peaks result from the change of the oxidation state of Fe in CrHCF, which in turn induces the intercalation and deintercalation of Na or K cations, respectively. Figure 2C shows typical scanning electron microscopy (SEM) images of graphene foam before (top) and after (bottom) CrHCF thin-film deposition. The substrate shows a branch-like structure, but after the deposition of CrHCF thin films, the structure appears to be homogeneously covered with the deposit and shows a smooth topology with an average feature size of about 166 nm. X-ray photoelectron spectroscopy (XPS) analysis of CrHCF thin films deposited on flat Pt electrodes (see Figure 2D) indicates the presence of all key elements, Fe, K, and Cr.

The presence of K-related peaks in the XPS data suggests that not all K^+ cations are removed from the CrHCF thin films during deintercalation (CrHCF is in the deintercalated state, Figure 2D). The investigation of Fe $2p_{1/2}$ and Fe $2p_{3/2}$ peaks reveals that the main oxidation state of iron after deintercalation is +3 (at ∼713.39 and ∼727.13 eV for Fe $2p_{3/2}$ and Fe $2p_{1/2}$, respectively); also, the peaks with less peak area and reduced binding energy can be observed alongside these peaks (at ∼711.99 and ∼724.91 eV for Fe $2p_{3/2}$ and Fe $2p_{1/2}$, respectively).

According to Yamashita and Hayes,[23] these peaks can be assigned to Fe^{II}, caused by partially divergent oxidation of Fe during the K deintercalation process. Therefore, the tentative reaction scheme for intercalation/deintercalation of K ions in CrHCF thin films can be proposed as following

$$KCr^{II}[Fe^{III}(CN)_6] + K^+ + e^- \leftrightarrow K_2Cr^{II}[Fe^{II}(CN)_6] \quad (1)$$

According to recent studies,[13,18,24] anions participate in the intercalation/deintercalation processes and affect the reversibility and stability of the electrode materials. The influence of

DOI: 10.1021/acsomega.8b00273
ACS Omega 2018, 3, 5111−5115

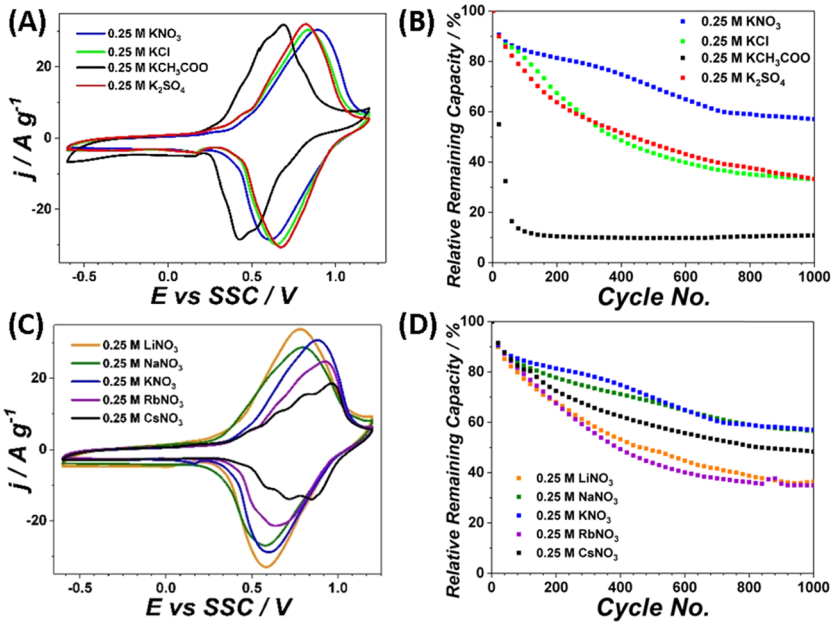

Figure 3. Characterization of the CrHCF electrodes in aqueous electrolytes containing different anions and/or alkali metal cations. (A) Typical CVs of CrHCF electrodes and (B) their long-term cycling tests in 0.25 M KNO_3 (blue), 0.25 M KCl (green), 0.25 M KOAc (black), and 0.25 M K_2SO_4 (red). (C) Typical CVs of CrHCF thin films and (D) their long-term cycling tests in 0.25 M $LiNO_3$ (yellow), 0.25 M $NaNO_3$ (olive), 0.25 M KNO_3 (blue), 0.25 M $RbNO_3$ (purple), and 0.25 M $CsNO_3$ (black).

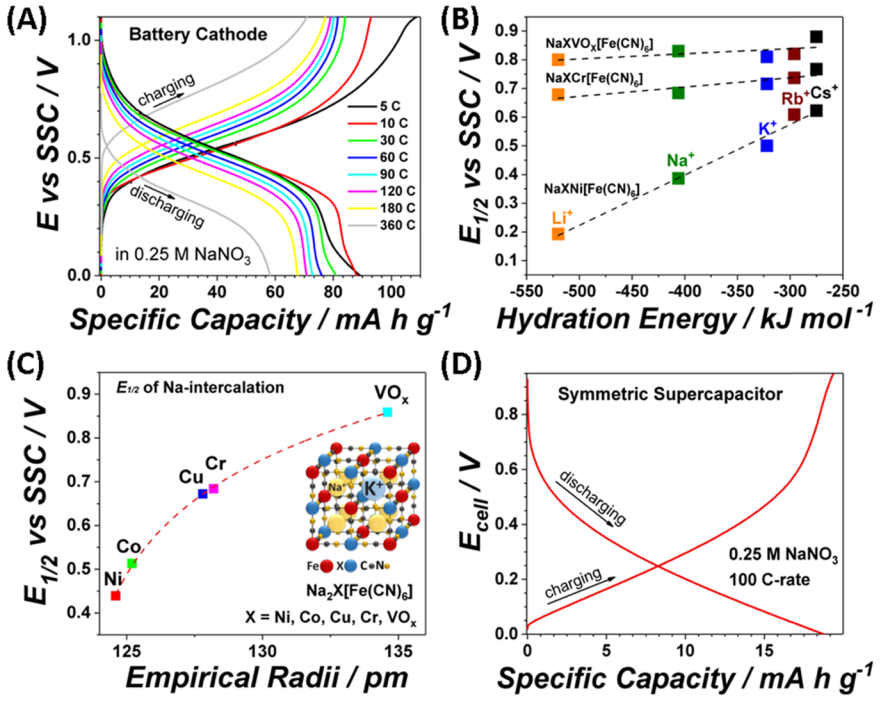

Figure 4. (A) Galvanostatic charge−discharge test of the CrHCF electrodes in 0.25 M $NaNO_3$ electrolytes at different C rates. (B) Comparison of the $E_{1/2}$ potentials for the CrHCF, VHCF, and NiCHF electrodes as a function of the hydration energy of the intercalating alkali metal cations. (C) $E_{1/2}$ potentials of NiHCF, CoHCF, CuHCF, VHCF, and CrHCF electrodes for Na intercalation/deintercalation as a function of empirical radii of transition metals.[17,26] (D) Charge−discharge characteristic curves for a CrHCF symmetric cell (quasi-supercapacitor) at 100 C using a 0.25 M $NaNO_3$ aqueous electrolyte.

the electrolyte composition on the reversibility and stability of CrHCF thin films was investigated using 0.25 M K-containing electrolytes, namely KNO_3, KCl, KOAc (potassium acetate), and K_2SO_4.

The shapes of CVs look similar regardless of the anions present in the electrolytes, whereas the potential of K intercalation/deintercalation varies (see Figure 3A). Among the studied electrolytes, the long-term stability tests of CrHCF electrodes showed the highest cycle stability in 0.25 M KNO_3 solutions (ca. 57% of the initial capacity), as shown in Figure 3B. The worst stability was observed for the sample in 0.25 M KOAc, which retained only ∼21% of its initial charge capacity

DOI: 10.1021/acsomega.8b00273
ACS Omega 2018, 3, 5111−5115

Table 1. Specific Capacities for CrHCF Electrodes in 0.25 M $NaNO_3$ at Different C-Rates

C-rate	5 C	10 C	30 C	60 C	90 C	120 C	180 C	360 C
specific capacity (mA h/g)	~89	~88	~81	~76	~73	~71	~68	~58

after only 50 cycles. The large channels of PBAs have been shown to be able to host different cations.[13,25] Figure 3C shows the CVs of CrHCF thin films in 0.25 M XNO_3 electrolytes (X = Li, Na, K, Rb, and Cs) characterizing quasi-reversible intercalation/deintercalation of different alkali metal cations into/from CrHCF. The shapes of CVs in different electrolytes appear similar except for the case of 0.25 M $CsNO_3$, but the positions of the CVs are slightly different. Subsequently, the long-term cycling tests of CrHCF thin films were performed in different electrolytes for 1000 cycles (see Figure 3D). CrHCF thin films cycled in $NaNO_3$ and KNO_3 showed the best stabilities after 1000 cycles, reaching ~56 and ~57% of the initial capacity, respectively.

The specific capacity of a CrHCF electrode in 0.25 M $NaNO_3$ was measured at multiple C rates to investigate the rate performance (see Figure 4A). The resulting specific capacities strongly depended on the applied C rate (summarized in Table 1). At 10 C, the electrode showed a specific capacity of ~88 mA h/g, and the specific capacities tend to be lower at higher C rates. The half-charge potential ($E_{1/2}$) of CrHCF thin films slightly varies depending on the nature of the alkali metal cations in different electrolytes as shown in Figure 4B.

In contrast to the case of NiHCF,[13] the half-charge potentials of CrHCF only slightly depend on the hydration energy of alkali metal cations, similar to VHCF.[17] Figure 4C shows a good correlation between the $E_{1/2}$ potentials for different PBAs (NiHCF, CoHCF, CuHCF, VHCF, and CrHCF) and the empirical radii of the key TM^1 elements of PBAs. The larger the empirical radii of the transition metals TM^1 in PBAs, the higher the $E_{1/2}$ potentials are.

Using CrHCF, we have also constructed a symmetric cell (quasi-supercapacitor with two identical CrHCF electrodes) operating at 100 C, with the maximum initial operational voltage of 0.95 V (see Figure 4D). It demonstrated a specific capacity of ~19 mA h/g and a specific energy density of ~4.6 W h/kg. At 120 C, the Coulombic efficiency exhibited ~99.6%. These values slightly outperform those of commercially available nonaqueous supercapacitor systems for power grids and industrial applications (energy density of ~3−4 W h/kg and maximum efficiency at nominal power of 98.6%).[27,28]

The good rate performance of CrHCF electrodes would position them between battery and supercapacitor materials, opening the possibility of future application of this material in hybrid ESSs. If the CrHCF electrode is combined with an appropriate Na battery anode, such as a phosphorene−graphene anode,[29] the recently reported high-rate TiO_2 anode,[30] or MnHCM,[18] it would result in a full cell with excellent voltage and rate capability.

CONCLUSIONS

In summary, we have demonstrated electrodeposited CrHCF thin films as an affordable cathode material for aqueous Na^+ and K^+ ion batteries. CrHCF electrodes exhibited the $E_{1/2}$ potential of ~0.69 and ~0.72 V versus SSC for Na and K intercalation, respectively, and a high specific capacity of ~88 mA h/g at 10 C, with excellent cycling stability and capacity retention of ~60% after 1000 cycles. Surprisingly, the choice of electrolytes has a significant influence on the cycle life. The electrode potential of PBAs appears to be adjustable by replacing N-coordinated transition metals with others. The symmetric cell using two CrHCF electrodes showed a high voltage of 0.95 V and an energy density of ~4.6 W h/kg at 100 C. The high availability of raw resources for the fabrication of CrHCF electrodes should enable the use of this material in large-scale ESSs.

EXPERIMENTAL SECTION

Electrochemical measurements were carried out in an electrochemical glass cell in Ar-saturated electrolytes (Argon 5.0 Westfalen AG) using a three-electrode configuration and a VSP-300 potentiostat (Bio-Logic, France) to control the experiments. Graphene/thermoplastic polyurethane flexible foam (Graphene Supermarket, USA) and AT-cut Pt quartz crystals (Standford Research Systems, USA) served as working electrodes and substrates, respectively, for the electrochemical deposition of CrHCF thin films. A Pt wire and 3 M KCl Ag/AgCl (SSC, Schott) were used as a counter and a reference electrode, respectively. The electrochemical deposition of CrHCF thin films was performed using a deposition solution containing 0.25 M KNO_3, 10 mM $CrCl_3$ (prepared from $CrCl_3 \cdot 6H_2O$, 95%, Sigma-Aldrich, Germany), and 5 mM $K_3Fe[(CN)_6]$ (~99%, ReagentPlus, Sigma-Aldrich, Germany) in ultrapure water (Evoqua, Germany) by cycling electrode potential between −1.1 and 1.25 V versus SSC at a scan rate of 50 mV s^{-1}. Cyclic voltammetry analysis of the resulting CrHCF thin films was performed in different electrolytes (0.25 M KNO_3, 0.25 M KCl, 0.25 M K_2SO_4, 0.25 M KCH_3COO, 0.25 M $LiNO_3$, 0.25 M $NaNO_3$, 0.25 M KNO_3, 0.25 M $RbNO_3$, and 0.25 M $CsNO_3$, all ReagentPlus, Sigma-Aldrich, Germany) to investigate the electrochemical characteristics and battery performance. For that, the electrode potential was cycled from −0.6 to 1.2 V versus SSC for 1000 cycles at a rate of 50 mV s^{-1}. Battery capacitance determination tests of CrHCF thin films were carried out in the 0.25 M $NaNO_3$ electrolyte at different C rates (5, 10, 30, 60, 90, 120, 180, and 360 C). A 0.95 V symmetric cell (a quasi-supercapacitor) was constructed using two CrHCF thin-film electrodes and the 0.25 M $NaNO_3$ aqueous electrolyte; and its charge−discharge test was performed at 100 C. Prior to the XPS measurements, the electrochemically deposited CrHCF thin films were rinsed with pure water several times to remove possible residues of still-adsorbed chemicals and then dried in ambient conditions. It should be noted here that the drying procedure in ambient conditions did not introduce any functional changes of the CrHCF thin films, neither in electrochemical nor XPS measurements. The XPS setup included SPECS GmbH XR50 X-ray source with Al anode (Kα line at 1486.61 eV), a SPECS GmbH spectrometer, and SPECS GmbH PHOIBOS 150 hemispherical energy analyzer. High-resolution field emission SEM analysis of the deposited films was performed on Zeiss NVision 40, operated at 3 kV.

AUTHOR INFORMATION

Corresponding Author

*E-mail: bandarenka@ph.tum.de. Phone: +49 (0) 89 289 12531 (A.S.B.).

DOI: 10.1021/acsomega.8b00273
ACS Omega 2018, 3, 5111−5115

ORCID
Philipp Marzak: 0000-0003-3372-0816
Aliaksandr S. Bandarenka: 0000-0002-5970-4315

Notes

The authors declare no competing financial interest.

■ ACKNOWLEDGMENTS

Financial support from the cluster of excellence Nanosystems Initiative Munich (NIM) and the TUM-IGSSE project 11.01 is gratefully acknowledged. J.Y. is thankful for the financial support from Nagelschneider Stiftung. This work was supported by the German Research Foundation (DFG) and the Technical University of Munich within the Open Access Publishing Funding Programme.

■ REFERENCES

(1) Nykvist, B.; Nilsson, M. Rapidly Falling Costs of Battery Packs for Electric Vehicles. *Nat. Clim. Change* **2015**, *5*, 329−332.
(2) Béguin, F.; Presser, V.; Balducci, A.; Frackowiak, E. Carbons and Electrolytes for Advanced Supercapacitors. *Adv. Mater.* **2014**, *26*, 2219−2251.
(3) Block, D.; Harrison, J. *Electric Vehicle Sales and Future Projections*; Electric Vehicle Transportation Center: Cocoa, FL, Jan 2014.
(4) Malhotra, A.; Battke, B.; Beuse, M.; Stephan, A.; Schmidt, T. Use Cases for Stationary Battery Technologies: A Review of the Literature and Existing Projects. *Renewable Sustainable Energy Rev.* **2016**, *56*, 705−721.
(5) Vesborg, P. C. K.; Jaramillo, T. F. Addressing the Terawatt Challenge: Scalability in the Supply of Chemical Elements for Renewable Energy. *RSC Adv.* **2012**, *2*, 7933−7947.
(6) Dunn, B.; Kamath, H.; Tarascon, J.-M. Electrical Energy Storage for the Grid: A Battery of Choices. *Science* **2011**, *334*, 928−935.
(7) Sonoc, A.; Jeswiet, J. A Review of Lithium Supply and Demand and a Preliminary Investigation of a Room Temperature Method to Recycle Lithium Ion Batteries to Recover Lithium and Other Materials. *Procedia CIRP* **2014**, *15*, 289−293.
(8) Kim, H.; Hong, J.; Park, K.-Y.; Kim, H.; Kim, S.-W.; Kang, K. Aqueous Rechargeable Li and Na Ion Batteries. *Chem. Rev.* **2014**, *114*, 11788−11827.
(9) Lu, Y.; Wang, L.; Cheng, J.; Goodenough, J. B. Prussian Blue: a New Framework of Electrode Materials for Sodium Batteries. *Chem. Commun.* **2012**, *48*, 6544−6546.
(10) Xue, L.; Li, Y.; Gao, H.; Zhou, W.; Lü, X.; Kaveevivitchai, W.; Manthiram, A.; Goodenough, J. B. Low-Cost High-Energy Potassium Cathode. *J. Am. Chem. Soc.* **2017**, *139*, 2164−2167.
(11) Pasta, M.; Wessells, C. D.; Huggins, R. A.; Cui, Y. A High-rate and Long Cycle Life Aqueous Electrolyte Battery for Grid-scale Energy Storage. *Nat. Commun.* **2012**, *3*, 1149.
(12) Wessells, C. D.; Peddada, S. V.; Huggins, R. A.; Cui, Y. Nickel Hexacyanoferrate Nanoparticle Electrodes for Aqueous Sodium and Potassium Ion Batteries. *Nano Lett.* **2011**, *11*, 5421−5425.
(13) Yun, J.; Pfisterer, J.; Bandarenka, A. S. How Simple Are the Models of Na Intercalation in Aqueous Media? *Energy Environ. Sci.* **2016**, *9*, 955−961.
(14) Senthilkumar, S. T.; Abirami, M.; Kim, J.; Go, W.; Hwang, S. M.; Kim, Y. Sodium-ion Hybrid Electrolyte Battery for Sustainable Energy Storage Applications. *J. Power Sources* **2017**, *341*, 404−410.
(15) Pasta, M.; Wang, R. Y.; Ruffo, R.; Qiao, R.; Lee, H.-W.; Shyam, B.; Guo, M.; Wang, Y.; Wray, L. A.; Yang, W.; Toney, M. F.; Cui, Y. Manganese−Cobalt Hexacyanoferrate Cathodes for Sodium-Ion Batteries. *J. Mater. Chem. A* **2016**, *4*, 4211−4223.
(16) Wessells, C. D.; Huggins, R. A.; Cui, Y. Copper Hexacyanoferrate Battery Electrodes with Long Cycle Life and High Power. *Nat. Commun.* **2011**, *2*, 550.
(17) Paulitsch, B.; Yun, J.; Bandarenka, A. S. Electrodeposited $Na_2VO_x[Fe(CN)_6]$ Films as a Cathode Material for Aqueous Na-Ion Batteries. *ACS Appl. Mater. Interfaces* **2017**, *9*, 8107−8112.
(18) Yun, J.; Schiegg, F. A.; Liang, Y.; Scieszka, D.; Garlyyev, B.; Kwiatkowski, A.; Wagner, T.; Bandarenka, A. S. Electrochemically Formed Na_xMn [Mn $(CN)_6$] Thin Film Anodes Demonstrate Sodium Intercalation and De-Intercalation at Extremely Negative Electrode Potentials in Aqueous Media. *ACS Appl. Energy Mater.* **2018**, *1*, 123−128.
(19) Lee, H.-W.; Wang, R. Y.; Pasta, M.; Lee, S. W.; Liu, N.; Cui, Y. Manganese Hexacyanomanganate Open Framework as a High-Capacity Positive Electrode Material for Sodium-Ion Batteries. *Nat. Commun.* **2014**, *5*, 5280.
(20) Gao, Z. Electrochemical Behavior of Chromium(III)-Hexacyanoferrate Film Modified Electrodes: Voltammetric and Electrochemical Impedance Studies. *J. Electroanal. Chem.* **1994**, *370*, 95−102.
(21) Jiang, M.; Zhou, X.; Zhao, Z. A New Zeolitic Thin Film Based on Chromium Hexacyanoferrate on Conducting Substrates. *J. Electroanal. Chem. Interfacial Electrochem.* **1990**, *287*, 389−394.
(22) Bratsch, S. G. Standard Electrode Potentials and Temperature Coefficients in Water at 298.15 K. *J. Phys. Chem. Ref. Data* **1989**, *18*, 1−21.
(23) Yamashita, T.; Hayes, P. Analysis of XPS Spectra of Fe^{2+} and Fe^{3+} Ions in Oxide Materials. *Appl. Surf. Sci.* **2008**, *254*, 2441−2449.
(24) Ventosa, E.; Paulitsch, B.; Marzak, P.; Yun, J.; Schiegg, F.; Quast, T.; Bandarenka, A. S. The Mechanism of the Interfacial Charge and Mass Transfer during Intercalation of Alkali Metal Cations. *Adv. Sci.* **2016**, *3*, 1600211.
(25) Wang, R. Y.; Wessells, C. D.; Huggins, R. A.; Cui, Y. Highly Reversible Open Framework Nanoscale Electrodes for Divalent Ion Batteries. *Nano Lett.* **2013**, *13*, 5748−5752.
(26) Teatum, E.; Gschneider, K.; Waber, J. *Report NoLA-2345*; U.S. Dept. of Commerce: Washington, D.C., 1960; p 45.
(27) Grid-Scale Energy Storage System for Back-Up Power and Power Quality Applications. https://www.skeletontech.com/skelgrid (accessed March 30, 2018).
(28) Skeleton Module 170V SMOD170V53F Datasheet, 2016. https://www.skeletontech.com/hubfs/Skeleton-170Vmodule_datasheet.pdf (accessed Mar 30, 2018), Skeleton Technologies GmbH.
(29) Sun, J.; Lee, H.-W.; Pasta, M.; Yuan, H.; Zheng, G.; Sun, Y.; Li, Y.; Cui, Y. A Phosphorene−Graphene Hybrid Material as a High-Capacity Anode for Sodium-Ion Batteries. *Nat. Nanotechnol.* **2015**, *10*, 980−985.
(30) Zhou, M.; Xu, Y.; Wang, C.; Li, Q.; Xiang, J.; Liang, L.; Wu, M.; Zhao, H.; Lei, Y. Amorphous TiO_2 Inverse Opal Anode For High-Rate Sodium Ion Batteries. *Nano Energy* **2017**, *31*, 514−524.

DOI: 10.1021/acsomega.8b00273
ACS Omega 2018, 3, 5111−5115